

## Metal-Organic Framework from an Anthracene Derivative Containing Nanoscopic Cages Exhibiting High Methane Uptake

Shengqian Ma,<sup>†</sup> Daofeng Sun,<sup>†</sup> Jason M. Simmons,<sup>‡,§</sup> Christopher D. Collier,<sup>†</sup> Daqiang Yuan,<sup>†</sup> and Hong-Cai Zhou<sup>\*,†</sup>

Department of Chemistry and Biochemistry, Miami University, Oxford, Ohio, 45056, NIST Center for Neutron Research, National Institute of Standards and Technology, Gaithersburg, Maryland 20899-6102, and Department of Materials Science and Engineering, University of Pennsylvania, Philadelphia, Pennsylvania 19104

Received September 18, 2007; E-mail: zhouh@muohio.edu

**Abstract:** A microporous metal-organic framework, PCN-14, based on an anthracene derivative, 5,5'-(9,10-anthracenediyl)di-isophthalate (H<sub>4</sub>adip), was synthesized under solvothermal reaction conditions. X-ray single crystal analysis revealed that PCN-14 consists of nanoscopic cages suitable for gas storage. N<sub>2</sub>-adsorption studies of PCN-14 at 77 K reveal a Langmuir surface area of 2176 m<sup>2</sup>/g and a pore volume of 0.87 cm<sup>3</sup>/g. Methane adsorption studies at 290 K and 35 bar show that PCN-14 exhibits an absolute methane-adsorption capacity of 230 v/v, 28% higher than the DOE target (180 v/v) for methane storage.

### 1. Introduction

Ongoing efforts<sup>3</sup> have been made in the search for alternative fuels to supplement or replace widely used gasoline and diesel fuels in vehicular applications. Among various alternative fuels, methane stands out when its profusion and availability are considered.<sup>1</sup> However, the lack of an effective, economic, and safe on-board storage system is one of the major technical barriers preventing methane-driven automobiles from competing with the traditional ones. To promote the vehicular application of methane, the U.S. Department of Energy (DOE) has set the target for methane storage at 180 v(STP)/v (standard temperature and pressure equivalent volume of methane per volume of the adsorbent material) under 35 bar, near ambient temperature, with the energy density of adsorbed natural gas (ANG) being comparable to that of compressed natural gas (CNG) used in current practice.<sup>2</sup>

Several types of porous materials including single-walled carbon nanotubes,<sup>3</sup> zeolites,<sup>4</sup> and activated carbon<sup>5</sup> have been extensively tested and evaluated as potential storage media for methane. However, the DOE targets for methane storage remain illusive despite significant progress in activated carbon materials.<sup>6</sup>

Emerging as a new type of porous materials, metal-organic frameworks (MOFs)<sup>7</sup> have become a burgeoning field of

research in the past decade due to their interesting structures and various potential applications.<sup>8</sup> In particular, their exceptionally high surface areas,<sup>9</sup> uniform but tunable pore sizes,<sup>10</sup> and functionalizable pore walls<sup>11</sup> make MOFs suitable for methane storage and a number of other applications. Several

<sup>†</sup> Miami University.

<sup>‡</sup> National Institute of Standards and Technology.

<sup>§</sup> University of Pennsylvania.

(1) U.S. Energy Policy Act of 1992 (EPAct).

(2) Burchell, T.; Rogers, M. *SAE Tech. Pap. Ser.* **2000**, 2000-01-2205.

(3) Muris, M.; Dupont-Pavlovsky, N.; Bienfait, M.; Zeppenfeld, P. *Surf. Sci.* **2001**, *492*, 67.

(4) Dunn, J. A.; Rao, M.; Sircar, S.; Gorte, R. J.; Myers, A. L. *Langmuir* **1996**, *12*, 5896.

(5) Quinn, D. F.; MacDonald, J. A. F. *Carbon* **1992**, *29*, 1097.

(6) (a) Wegrzyn, J.; Gurevich, M. *Appl. Energy* **1996**, *55*, 71. (b) NSF press release (#07-011) [http://www.nsf.gov/news/news\\_summ.jsp?cntn\\_id=108390](http://www.nsf.gov/news/news_summ.jsp?cntn_id=108390).

(7) (a) Eddaoudi, M.; Moler, D. B.; Li, H.; Chen, B.; Reineke, T. M.; O'Keeffe, M.; Yaghi, O. M. *Acc. Chem. Res.* **2001**, *34*, 319. (b) Janiak, C. *J. Chem. Soc., Dalton Trans.* **2003**, 2781. (c) Rowsell, J. L. C.; Yaghi, O. M. *Microporous Mesoporous Mater.* **2004**, *73*, 3. (d) Hill, R. J.; Long, D.-L.; Champness, N. R.; Hubberstey, P.; Schröder, M. *Acc. Chem. Res.* **2005**, *38*, 335. (e) Lin, W. B. *J. Solid State Chem.* **2005**, *178*, 2486. (f) Ockwig, N. W.; Delgado-Friedrichs, O.; O'Keeffe, M.; Yaghi, O. M. *Acc. Chem. Res.* **2005**, *38*, 176.

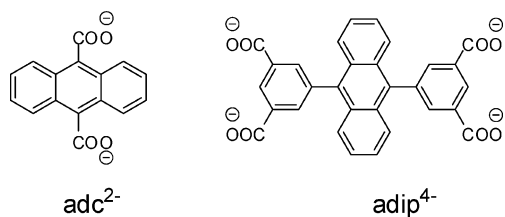
(8) (a) Seo, J. S.; Whang, D.; Lee, H.; Jun, S. I.; Oh, J.; Jeon, Y. J.; Kim, K. *Nature* **2000**, *404*, 982. (b) Rowsell, J. L. C.; Yaghi, O. M. *Angew. Chem., Int. Ed.* **2005**, *44*, 4670. (c) Matsuda, R.; Kitaura, R.; Kitagawa, S.; Kubota, Y.; Belosludov, R. V.; Kobayashi, T. C.; Sakamoto, H.; Chiba, T.; Takata, M.; Kawazoe, Y.; Mita, Y. *Nature* **2005**, *436*, 238. (d) Sun, D.; Ma, S.; Ke, Y.; Petersen, T. M.; Zhou, H.-C. *Chem. Commun.* **2005**, 2663. (e) Sun, D.; Ke, Y.; Mattox, T. M.; Ooro, B. A.; Zhou, H.-C. *Chem. Commun.* **2005**, 5447. (f) Sun, D.; Ma, S.; Ke, Y.; Collins, D. J.; Zhou, H.-C. *J. Am. Chem. Soc.* **2006**, *128*, 3896. (g) Ma, S.; Zhou, H.-C. *J. Am. Chem. Soc.* **2006**, *128*, 11734. (h) Ma, S.; Sun, D.; Ambrogio, M. W.; Fillinger, J. A.; Parkin, S.; Zhou, H.-C. *J. Am. Chem. Soc.* **2007**, *129*, 1858. (i) Sun, D.; Ke, Y.; Mattox, T. M.; Parkin, S.; Zhou, H.-C. *Inorg. Chem.* **2006**, *45*, 7566. (j) Sun, D.; Collins, D. J.; Ke, Y.; Zuo, J.-L.; Zhou, H.-C. *Chem.-Eur. J.* **2006**, *12*, 3768. (k) Ma, S.; Wang, X.-S.; Manis, E. S.; Collier, C. D.; Zhou, H.-C. *Inorg. Chem.*, **2007**, *46*, 3432. (l) Ma, S.; Sun, D.; Wang, X.-S.; Zhou, H.-C. *Angew. Chem., Int. Ed.* **2007**, *46*, 2458. (m) Collins, D. J.; Zhou, H.-C. *J. Mater. Chem.* **2007**, *17*, 3154. (n) Yu, C.; Ma, S.; Pechan, M. J.; Zhou, H.-C. *J. Appl. Phys.* **2007**, *101*, 09E108. (o) Gu, J.-Z.; Lu, W.-G.; Zhou, H.-C.; Lu, T.-B. *Inorg. Chem.* **2007**, *46*, 5835. (p) Sun, D.; Ke, Y.; Collins, D. J.; Lorigan, G. A.; Zhou, H.-C. *Inorg. Chem.* **2007**, *46*, 2725.

(9) (a) Chae, H. K.; Siberio-Perez, D. Y.; Kim, J.; Go, Y. B.; Eddaoudi, M.; Matzger, A. J.; O'Keeffe, M.; Yaghi, O. M. *Nature* **2004**, *427*, 523. (b) Ferey, G.; Mellot-Draznieks, C.; Serre, C.; Millange, F.; Dutour, J.; Surlbe, S.; Margiolaki, I. *Science* **2005**, *309*, 2040.

(10) (a) Eddaoudi, M.; Kim, J.; Rosi, N.; Vodak, D.; Wachter, J.; O'Keeffe, M.; Yaghi, O. M. *Science* **2002**, *295*, 469. (b) Chen, B.; Ma, S.; Zapata, F.; Lobkovsky, E. B.; Yang, J. *Inorg. Chem.* **2006**, *45*, 5718. (c) Chen, B.; Ma, S.; Zapata, F.; Fronczek, F. R.; Lobkovsky, E. B.; Zhou, H.-C. *Inorg. Chem.* **2007**, *46*, 1233.

(11) (a) Kitagawa, S.; Kitaura, R.; Noro, S.-i. *Angew. Chem., Int. Ed.* **2004**, *43*, 2334. (b) Wang, X.-S.; Ma, S.; Sun, D.; Parkin, S.; Zhou, H.-C. *J. Am. Chem. Soc.* **2006**, *128*, 16474. (c) Bradshaw, D.; Claridge, J. B.; Cussen, E. J.; Prior, T. J.; Rosseinsky, M. J. *Acc. Chem. Res.* **2005**, *38*, 273.

Scheme 1. Carboxylate Linkers



porous MOFs have been screened for methane storage but none have reached the DOE target.<sup>10a,12</sup> A recent computational study indicated that aromatic rings in MOFs can improve the methane-binding energy, enhancing both the uptake and the heat of methane-adsorption.<sup>13</sup>

Recently, a theoretically proposed MOF (IRMOF-993) based on 9,10-anthracene-dicarboxylate (adc) (Scheme 1) was predicted to have a methane adsorption capacity of 181 v(STP)/v, surpassing the DOE target.<sup>13</sup> However, experiments in our laboratory using 9,10-anthracene-dicarboxylate have led to an ultramicroporous MOF (PCN-13, PCN stands for Porous Coordination Network) with very limited methane uptake (see Supporting Information Figure S1). Instead, PCN-13 exhibits selective adsorption of hydrogen and oxygen over nitrogen and carbon monoxide because of the confined pore size ( $\sim 3.5$  Å).<sup>14</sup> To enlarge the pore size and to continue our theme of building metal-organic frameworks containing nanoscopic coordination cages for gas storage,<sup>8f,g,h</sup> we have adopted a new ligand, 5,5'-(9,10-anthracenediyl)di-isophthalate (adip, Scheme 1). Under solvothermal reaction conditions, the reaction between H<sub>4</sub>adip and Cu(NO<sub>3</sub>)<sub>2</sub> gave rise to a porous MOF designated PCN-14. In this contribution, we describe the synthesis and characterization of H<sub>4</sub>adip and PCN-14 and the methane-adsorption studies of the MOF.

## 2. Experimental Section

**General Information.** Commercially available reagents were used as received without further purification. Elemental analyses (C, H, and N) were obtained by Canadian Microanalytical Service Ltd.<sup>15</sup> TGA was performed under N<sub>2</sub> on a Perkin-Elmer TGA 7 and a Beckman Coulter SA3100 surface area analyzer was used to measure gas adsorption. NMR data were collected on a Bruker 300 MHz spectrometer. XRPD patterns were obtained on a Scintag X1 powder diffractometer system using CuK<sub>α</sub> radiation with a variable divergent slit, solid-state detector, and a routine power of 1400 W (40 kV, 35 mA). Powder samples were dispersed on low-background quartz XRD slides (Gem Depot, Inc., Pittsburgh, Pennsylvania) for analyses.

**Synthesis of 5,5'-(9,10-Anthracenediyl)bis(1,3-benzenedimethoxy-carbonyl), 1.** Anthracene 9,10-diboronic acid (0.5 g, 0.002 mol), dimethyl-5-bromo-isophthalate (1.7 g, 0.006 mol) and Pd(PPh<sub>3</sub>)<sub>4</sub> (0.02 g) were mixed in a 500 mL flask. The flask was pumped under vacuum

for 30 min and 80 mL degassed THF was added. After the addition of 15 mL degassed 2 M Na<sub>2</sub>CO<sub>3</sub> solution, the mixture was heated to reflux under nitrogen atmosphere for 40 h. The resulting yellow mixture was diluted with water and extracted with CH<sub>2</sub>Cl<sub>2</sub> three times. The mixed organic phase was dried with MgSO<sub>4</sub>, and the solvent was removed to give a brown solid. The crude product was purified by column chromatography on silica gel with CHCl<sub>3</sub> as the eluent to give **1** as a yellow solid (0.6 g, 53%). <sup>1</sup>H NMR (CDCl<sub>3</sub>): δ = 8.9 (s, 2 H), 8.5 (s, 4 H), 7.6 (d, 4 H), 7.4 (m, 4 H), 4.0 (s, 12 H).

**Synthesis of H<sub>4</sub>adip, 5,5'-(9,10-Anthracenediyl)di-isophthalic Acid, 2.** Compound **1** (0.6 g, 0.001 mol) was suspended in 50 mL of THF, to which 10 mL of a 2 M KOH aqueous solution was added. The mixture was stirred at room temperature overnight. THF was removed using a rotary evaporator, and diluted hydrochloric acid was added to the remaining aqueous solution until it became acidic. The solid was collected by filtration, washed with water several times, and dried to give **2** (0.4 g, 80%). <sup>1</sup>H NMR (CDCl<sub>3</sub>): δ = 13.5 (br, 4 H), 8.7 (s, 2 H), 8.2 (s, 4 H), 7.5 (m, 8 H).

**Synthesis of PCN-14, Cu<sub>2</sub>(H<sub>2</sub>O)<sub>2</sub>(adip)·2DMF.** A mixture of **2** (0.005 g, 1.4 × 10<sup>-5</sup> mol), Cu(NO<sub>3</sub>)<sub>2</sub>·2.5H<sub>2</sub>O (0.02 g, 8.2 × 10<sup>-6</sup> mol), and 2 drops of HBF<sub>4</sub> in 1.5 mL DMF was sealed in a Pyrex tube under vacuum and heated to 75 °C at a rate of 1 °C/min, kept at that temperature for 1 day, and cooled to room temperature at a rate of 0.1 °C/min. The resulting green block crystals were washed with DMF (yield: 75% based on **2**) and has a formula of Cu<sub>2</sub>(H<sub>2</sub>O)<sub>2</sub>(adip)·2DMF, which was derived from crystallographic data, elemental analysis (calcd: C, 49.94; H, 4.42; N, 3.24. Found: C, 51.03; H, 4.54; N, 3.15%), and TGA (Figure S2, Supporting Information).

**X-ray Crystallography.** Single-crystal X-ray structure determination of PCN-14 was performed on a specially configured diffractometer based on the Bruker-Nonius X8 Proteum using focused Cu-K<sub>α</sub> radiation (λ = 1.54178 Å). Raw data for all structures were processed using SAINT and absorption corrections were applied using SADABS.<sup>16</sup> The structures were solved by direct method and refined by full-matrix least-squares on F<sup>2</sup> with anisotropic displacement parameters for non-H atoms using SHELX-97.<sup>17</sup> The hydrogen atoms on the carbon were placed in calculated position with isotropic displacement parameters set to 1.2 × U<sub>eq</sub> of the attached atom. Solvent molecules in the structure were highly disordered and were impossible to refine using conventional discrete-atom models. To resolve these issues, the contribution of solvent electron density was removed by the SQUEEZE routine in PLATON.<sup>18</sup>

**Low-Pressure Nitrogen Sorption Measurements.** The low-pressure nitrogen adsorption measurements were performed at 77 K and 0–760 Torr on a Beckman Coulter SA 3100 surface area and pore size analyzer. An as-isolated sample of PCN-14 was immersed in methanol for 24 h, and the extract was decanted. Fresh methanol was subsequently added, and the crystals were allowed to stay for an additional 24 h to remove the nonvolatile solvates (DMF and H<sub>2</sub>O). The sample was collected by decanting and treated with dichloromethane similarly to remove methanol solvates. After the removal of dichloromethane by decanting, the sample was dried under a dynamic vacuum (<10<sup>-3</sup> Torr) at room temperature (25 °C) overnight. Before the measurement, the sample was dried again by using the “outgas” function of the surface area analyzer for 4 h at 120 °C. High purity nitrogen (99.999%) was used for the measurement. The regulator and pipe were flushed with nitrogen before connecting to the analyzer. The internal lines of the instrument were flushed three times by utilizing the “flushing lines” function of the program to ensure the purity of N<sub>2</sub>.

**High-Pressure Methane Sorption Measurements.** High-pressure methane sorption isotherm measurements on PCN-14 were performed

- (12) (a) Noro, S.-i.; Kitagawa, S.; Kondo, M.; Seki, K. *Angew. Chem., Int. Ed.* **2000**, *39*, 1433. (b) Kondo, M.; Shimamura, M.; Noro, S.-i.; Minakoshi, S.; Asami, A.; Seki, K.; Kitagawa, S. *Chem. Mater.* **2000**, *12*, 1288. (c) Kesanli, B.; Cui, Y.; Smith Milton, R.; Bittner Edward, W.; Bockrath Bradley, C.; Lin, W. *Angew. Chem., Int. Ed.* **2005**, *44*, 72. (d) Bourrelly, S.; Llewellyn, P. L.; Serre, C.; Millange, F.; Loiseau, T.; Férey, G. *J. Am. Chem. Soc.* **2005**, *127*, 13519.
- (13) Dueren, T.; Sarkisov, L.; Yaghi, O. M.; Snurr, R. Q. *Langmuir* **2004**, *20*, 2683.
- (14) Ma, S.; Wang, X.-S.; Collier, C. D.; Manis, E. S.; Zhou, H.-C. *Inorg. Chem.* **2007**, *46*, 8499.
- (15) Note: Certain commercial suppliers are identified in this paper to foster understanding. Such identification does not imply recommendation or endorsement by the National Institute of Standards and Technology, nor does it imply that the materials or equipment identified are necessarily the best available for the purpose.

- (16) SAINT+, version 6.22; Bruker Analytical X-Ray Systems, Inc.: Madison, WI, 2001.
- (17) Sheldrick, G. M. SHELX-97; Bruker Analytical X-Ray Systems, Inc.: Madison, WI, 1997.
- (18) Spek, A. L. *J. Appl. Crystallogr.* **2003**, *36*, 7.

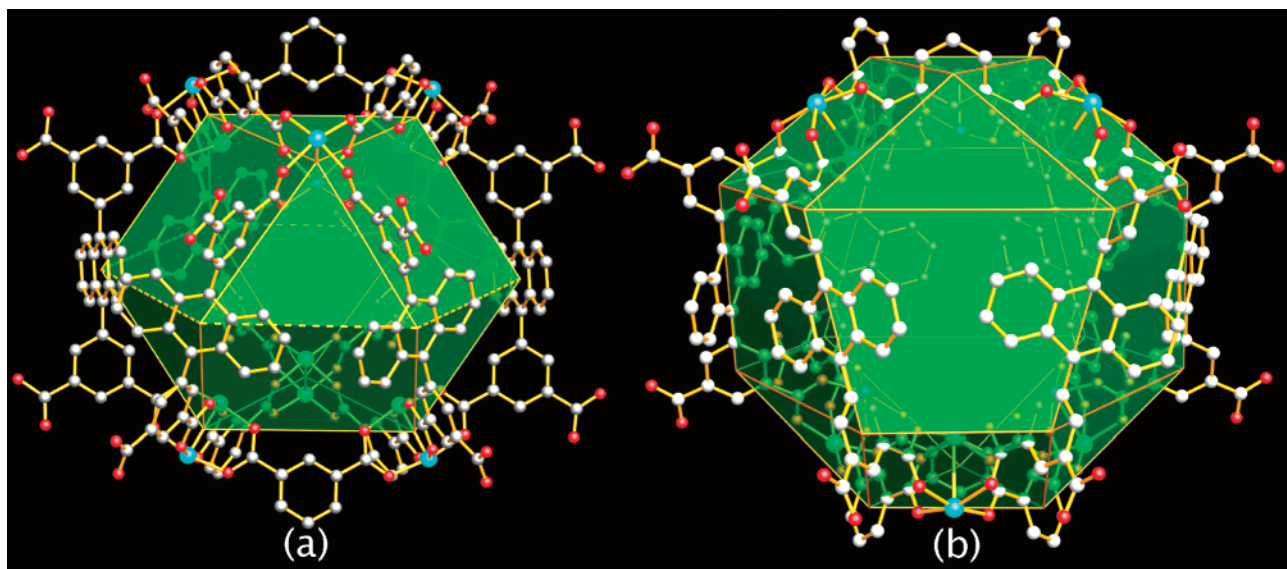


**Figure 1.** (a) Squashed cuboctahedral cage; (b) nanoscopic cage with 18 vertices, 30 edges, and 20 faces. Color scheme: C, gray; Cu, turquoise; and O, red.

using a home-built fully computer-controlled Sievert apparatus at NIST. The methane used for the high pressure measurements is scientific/research grade with the purity of 99.999%. The detailed specification of the Sievert apparatus and the data analysis can be found in a recently published work.<sup>19</sup> Briefly, the Sievert system is equipped with four high-precision gauges (0.1%) and a closed-cycle cryostat, enabling methane-adsorption measurements over a wide pressure (0–50 bar) and temperature (125–290 K) range. In all measurements, about 200 mg solvent-exchanged sample was used, which was activated under vacuum (less than  $10^{-4}$  Torr) in two stages: first heating at room temperature overnight, and then at 120 °C for at least 4 h. Once activated, the samples were transferred to He-glove box and never exposed to air.

**Excess Adsorption and Absolute Adsorption.** Details of excess adsorption and absolute adsorption have been described in a recently published work<sup>19</sup> as well as in some other published work.<sup>20</sup> In brief, the capacity of excess adsorption is the amount of adsorption gas interacting with the frameworks, whereas the capacity of absolute adsorption is the amount of gas both interacting with the frameworks and staying in pores in the absence of gas–solid intermolecular forces. For systems with known crystal structure, it is possible to directly measure the absolute adsorption in addition to excess adsorption.

### 3. Results and Discussion

**Structural Descriptions of PCN-14.** Single-crystal X-ray diffraction<sup>21</sup> revealed that PCN-14 crystallizes in the space group *R*-3*c*, different from those of previously reported [Cu<sub>2</sub>L(H<sub>2</sub>O)<sub>2</sub>] MOFs (L = biphenyl-3,3',5,5'-tetracarboxylate, terphenyl-3,3'',5,5'''-tetracarboxylate, or quaterphenyl-3,3''',5,5''''-tetracarboxylate),<sup>22</sup> which all crystallize in *R*-3*m* space group. PCN-14 consists of a dicopper paddlewheel secondary building unit

and the adip ligand. In the ligand, the four carboxylate groups and the two phenyl rings of the isophthalate motifs are almost in a plane, whereas the dihedral angle between the anthracene ring and the phenyl rings is 70.4°. Every 12 adip ligands connect 6 paddlewheel SBUs to form a squashed cuboctahedral cage (Figure 1a), if one connects the centers of the six paddlewheels and the six anthracenyl groups (broken lines in Figure 1a). The anthracenyl rings in the cage are in close contact (2.6 Å between an H atom and the center of a phenyl ring from the adjacent anthracenyl group). The cuboctahedral cage has eight triangular windows and six square windows for gas molecules to access the interior surface. The cuboctahedral cage can also be viewed as four intersecting hexagons. The dimensions of the hexagons are 9.23 Å along an edge and 18.45 between two opposite corners. Extending each hexagon in the cuboctahedral cage into two-dimensional honeycombs gives rise to a three-dimensional 4-connected net (Figure 2). The three-dimensional net can also be viewed as a framework consisting of cuboctahedral nanoscopic cages (Figure 3a). An alternative way of viewing the cage is to connect the centers of all isophthalate phenyl rings, forming a polygon with 18 vertices, 20 faces, and 30 edges. This polygon can be viewed as being formed by inserting an irregular hexagonal prism in between the two halves of a cuboctahedron (Figure 1b). The cage has 1150 Å<sup>3</sup> of void and is approximately spherical providing efficient and accessible interior surface for gas storage.

PCN-14 is very porous (Figure 3b). The solvent accessible volume for the desolvated PCN-14 is 63.5%, calculated using the PLATON routine,<sup>18</sup> comparable to those of other MOFs based on isophthalate derivatives.<sup>22a</sup>

**Low-Pressure Nitrogen Sorption.** A PCN-14 sample was fully activated by the procedure described above in the experimental section. The integrity of the framework was confirmed by powder X-ray diffraction (PXRD) before the nitrogen sorption measurements (Figure S3, Supporting Information). Nitrogen sorption isotherms of the fully activated PCN-14 sample (Figure 4) reveals typical Type-I sorption behavior, confirming the permanent porosity of the activated PCN-14. Calculated from the nitrogen adsorption data, the estimated BET

(19) Zhou, W.; Wu, H.; Hartman, M. R.; Yildirim, T. *J. Phys. Chem. C* **2007**, *111*, 16131.

(20) (a) Dincă, M.; Dailly, A.; Liu, Y.; Brown, C. M.; Neumann, D. A.; Long, J. R. *J. Am. Chem. Soc.* **2006**, *128*, 16876. (b) Furukawa, H.; Miller, M. A.; Yaghi, O. M. *J. Mater. Chem.* **2007**, *17*, 3197.

(21) X-ray crystal data for PCN-14: C<sub>270</sub>H<sub>162</sub>Cu<sub>18</sub>O<sub>90</sub>, fw = 5989.9, Rhombohedral, *R*-3*c*, *a* = 18.4530 (4) Å, *b* = 18.4530 (4) Å, *c* = 76.976(4) Å, *V* = 22699.7(1) Å<sup>3</sup>, *Z* = 2, *T* = 90 K, ρ<sub>calcd</sub> = 0.871 g/cm<sup>3</sup>, *R*<sub>1</sub> (*I* > 2σ(*I*)) = 0.0518, *wR*<sub>2</sub> (all data) = 0.1591, GOF = 1.071.

(22) (a) Chen, B. L.; Ockwig, N. W.; Millward, A. R.; Contreras, D. S.; Yaghi, O. M. *Angew. Chem., Int. Ed.* **2005**, *44*, 4745. (b) Lin, X.; Jia, J. H.; Zhao, X. B.; Thomas, K. M.; Blake, A. J.; Walker, G. S.; Champness, N. R.; Hubberstey, P.; Schröder, M. *Angew. Chem., Int. Ed.* **2006**, *45*, 7358.

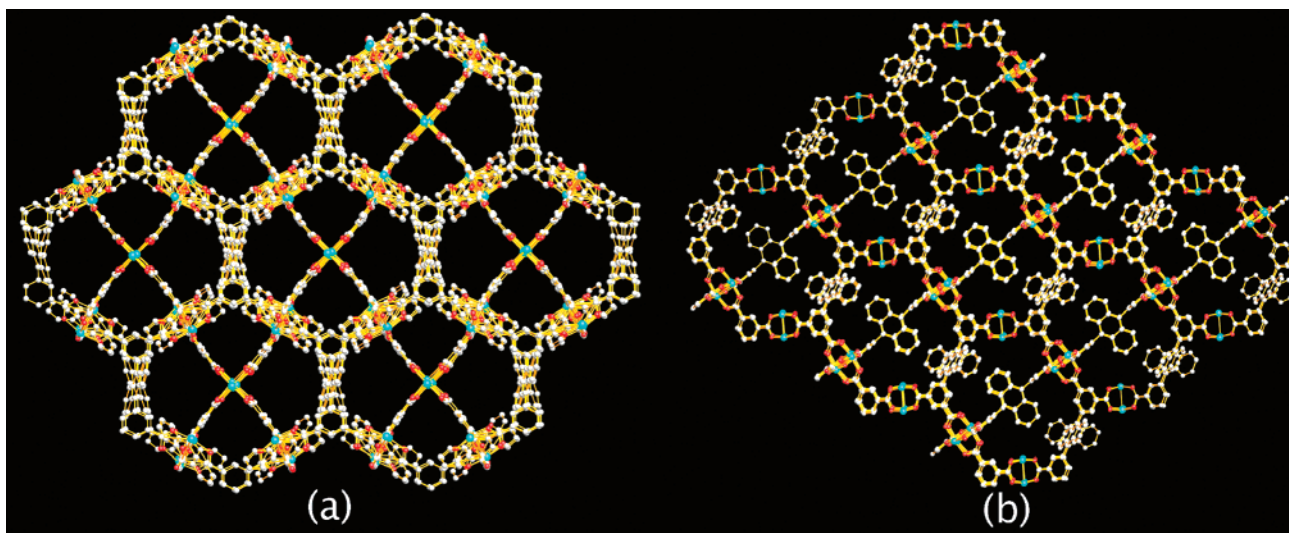


Figure 2. 3D framework of PCN-14 viewed from the (a) [2 1 1] and (b) [1 0 0] directions.

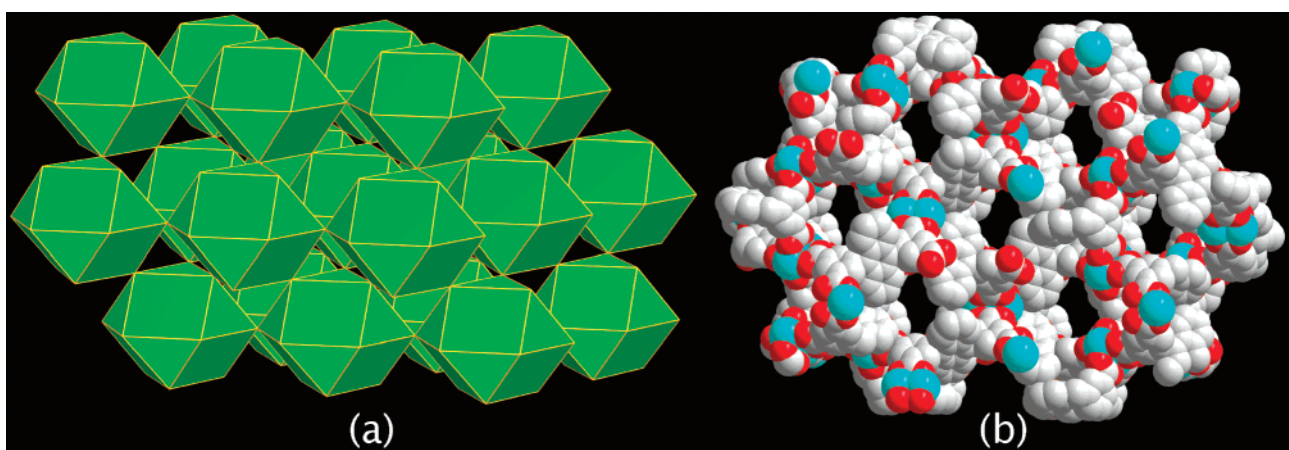


Figure 3. 3D framework of PCN-14 viewed as a (a) cuboctahedral net and (b) space filling model on the [1 0 3] plane.

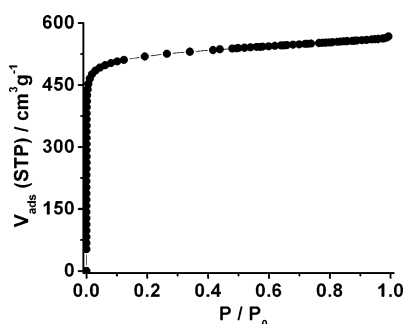


Figure 4. Nitrogen gas adsorption isotherm at 77 K.

surface area of PCN-14 is 1753 m<sup>2</sup>/g,<sup>23</sup> and the estimated pore volume is 0.87 cm<sup>3</sup>/g. These values are slightly higher than those of MOF-505 but lower than those of the two other MOFs using isophthalate derivatives.<sup>22</sup> Assuming monolayer coverage, PCN-14 has an estimated Langmuir surface area of 2176 m<sup>2</sup>/g.

**High-Pressure Methane Sorption.** High-pressure methane sorption measurements were performed at various temperatures to investigate the methane uptake. The methane uptake capacities were converted directly into v(STP)/v by using the crystallographic density of PCN-14 (0.871 g/cm<sup>3</sup>). As shown in Figure 5, the methane saturation uptake of both excess adsorption and

absolute adsorption decrease with increasing temperatures. The saturation of excess methane adsorption in PCN-14 at 125 K can reach 434 v(STP)/v, which corresponds to an adsorbed methane density of 310 mg/mL. The density is 73.4% of that of liquid methane (422.6 mg/mL) at 113 K.<sup>24</sup> At 290 K and 35 bar, the excess adsorption capacity of methane in PCN-14 is 220 v(STP)/v, corresponding to an absolute adsorption capacity of 230 v(STP)/v. The excess methane adsorption value is 22% higher than the DOE target of 180 v(STP)/v for methane.<sup>2</sup> To the best of our knowledge, PCN-14 exhibits the highest methane uptake capacity among reported porous materials for methane adsorption.<sup>12,13</sup>

**Analysis of Heat of Adsorption.** The strength of interactions between the framework and methane can be reflected by isosteric heats of adsorption  $Q_{st}$ . The isosteric heats of adsorption of methane were calculated using the Clausius-Clapeyron equation,<sup>25</sup>

$$Q_{st} = -R \cdot d(\ln P) / d(1/T)$$

using isotherms taken at 270, 280, and 290 K. As shown in

(24) Lide, D. R. *Handbook of Chemistry and Physics*, 73rd ed.; CRC Press, Inc.: Boca Raton, FL, 1992.

(25) Rouquerol, F.; Rouquerol, J.; Sing, K. *Adsorption by Powders and Solids: Principles, Methodology, and Applications*; Academic Press: London, 1999.

(23) Walton, K. S.; Snurr, R. Q. *J. Am. Chem. Soc.* **2007**, *129*, 8552.

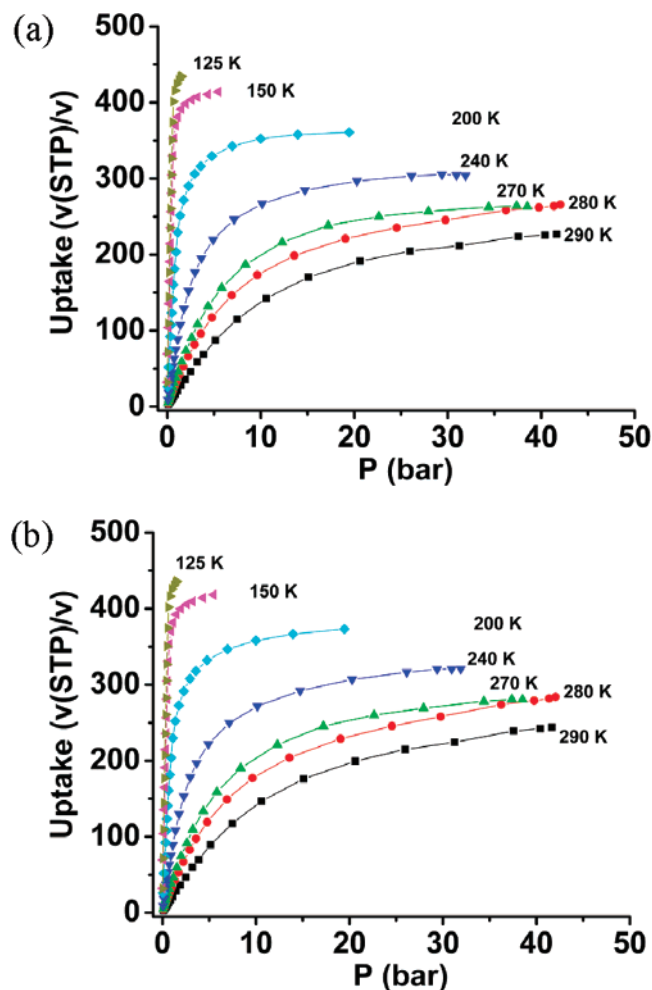


**Figure 5.** High-pressure methane sorption isotherms at various temperatures (a) excess adsorption; (b) absolute adsorption.

Figure 6, the  $Q_{st}$  at low loading is as high as 30 kJ/mol, revealing strong interactions between methane and the framework. The  $Q_{st}$  first slowly decreases and then increases gradually with the methane loading. This indicates that at high-concentration methane loading, the methane–methane interaction in addition to the methane–framework interaction becomes dominant as discovered in other MOFs systems.<sup>8g,19</sup> The high  $Q_{st}$  of PCN-14 is unprecedented in MOFs<sup>8g,12</sup> and supports the predictions

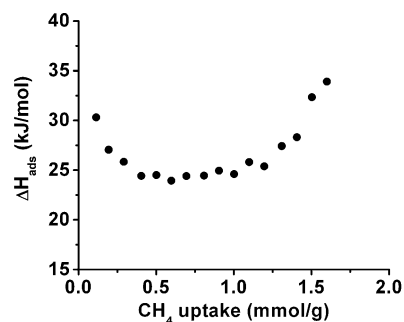


**Figure 6.** Isothermic heats of adsorption of methane.

that adding more aromatic rings to the ligand and incorporating nanoscopic cages to the framework can lead to higher affinity of methane.<sup>13</sup>

#### 4. Conclusions

In summary, a microporous MOF, PCN-14, based on a predesigned anthracene derivative, 5,5'-(9,10-anthracenediyl)-di-isophthalate, was synthesized and structurally characterized. It contains nanoscopic cages suitable for methane uptake.  $N_2$  adsorption measurements of PCN-14 at 77 K reveal an estimated Langmuir surface area of 2176  $m^2/g$  and an estimated pore volume of 0.87  $cm^3/g$ . High-pressure methane adsorption studies show that PCN-14 exhibits an absolute methane-adsorption capacity of 230 v/v (28% higher than the DOE target of 180 v/v at ambient temperatures) and heats of adsorption of methane of around 30 kJ/mol, both record highs among those reported for methane-storage materials.

**Acknowledgment.** This work was supported by the Department of Energy (DE-FC36-07GO17033) and the National Science Foundation (CHE-0449634). H.-C.Z. acknowledges Dr. Sean Parkin (the University of Kentucky) for single-crystal data collection and structure refinement of PCN-14, the Research Corporation for a Cottrell Scholar Award, and Air Products for a Faculty Excellence Award. J.M.S. also acknowledges support from DOE (BES DE-FG02-98ER45701).

**Supporting Information Available:** Crystallographic information file (CIF) of PCN-14, a TGA plot, and XPRD patterns are available free of charge via the Internet at <http://pubs.acs.org>.

JA0771639